

BSc Melanie Kaiser

**Study on the role of D-2-hydroxyglutarate on chromatin function
using the model organism *Saccharomyces cerevisiae***

MASTERARBEIT

zur Erlangung des akademischen Grades

Master of Science

Masterstudium Biochemie und Molekulare Biomedizin

eingereicht an der

Technischen Universität Graz

Betreuer

Prof. Kai-Uwe Fröhlich

Prof. Jasper Rine (UC Berkeley)

Dr. Ryan Janke (UC Berkeley)

Molecular Biosciences

Graz, November 2017

Eidesstattliche Erklärung

Ich erkläre an Eides statt, dass ich die vorliegende Arbeit selbstständig verfasst, andere als die angegebenen Quellen/Hilfsmittel nicht benutzt, und die den benutzten Quellen wörtlich und inhaltlich entnommenen Stellen als solche kenntlich gemacht habe.

Graz, am 15.11.2017

.....


(Unterschrift)

Statutory Declaration

I declare that I have authored this thesis independently, that I have not used other than the declared sources / resources, and that I have explicitly marked all material which has been quoted either literally or by content from the used sources.

Date 15.11.2017

.....


Preface

The content of this master's thesis was elaborated at *UC Berkeley's Rine Lab* between August 2016 and September 2017. *The Rine Lab*, led by Dr. Jasper Rine is a research institution with focus on gene regulation and cell biology in yeast *Saccharomyces cerevisiae*, contributing to a better understanding of the establishment, maintenance and epigenetic inheritance of silencing, as well as nutrition and heritable effects on gene expression and human nutritional genetics in general. Dr. Rine and his team frequently publish their results in top journals such as Science or Cell.

During this 13-month period, three projects in the field of epigenetics and silencing were pursued, as shown in table below.

Project Number	Title	Publication
1	Impact of D-2-hydroxyglutarate on silencing in regions other than <i>HML</i>	Poster presentation at Asilomar Conference grounds
2	Does knockout of <i>HMT1</i> and <i>MEU1</i> affect silencing at <i>HML</i> ?	-
3	Study on the role of D-2-hydroxyglutarate on chromatin function using the model organism <i>Saccharomyces cerevisiae</i>	In press

This thesis presents only the results of project number 3, “Study on the role of D-2-hydroxyglutarate on chromatin function using the model organism *Saccharomyces cerevisiae*”.

Abstract

The genetic code alone does not account for the entire range of phenotypes observed in nature. Epigenetics provides an additional layer of information that is not encoded in the DNA molecule but nonetheless influences its activity in a stable and heritable manner through cell division. Epigenetic pathways play a significant role in disease and the reversible nature of those aberrations has led to the emergence of the promising field of epigenetic therapy.

Mutations in NADP⁺-dependent isocitrate dehydrogenases (IDH1 and IDH2) occur in a variety of cancers in humans where they cause accumulation of the oncometabolite D-2-hydroxyglutarate (D-2-HG). D-2HG inhibits the TET DNA demethylases and Jumonji histone demethylases which leads to epigenetic alterations that drive cancer formation. Nevertheless D-2-HG is a metabolite found in all human body fluids and is maintained at low levels through the activity of D-2-hydroxyglutarate dehydrogenase (D2HGDH). The physiological role of D-2-HG is unknown, and its potential as a therapeutic target, emphasizes the need for further studies on this metabolite.

S. cerevisiae provided the opportunity to identify the full range of impacts D-2-HG has on an organism. Yeast strains with mutations in D-lactate dehydrogenase enzymes Dld2 and Dld3, orthologs of human D-lactate dehydrogenase D2HGDH, accumulated D-2-HG to levels comparable to those found in tumors. This property allowed the opportunity to screen for mutations that suppressed phenotypes caused by high levels of D-2-HG. Here, I report the identification of *RPD3*, *SIN3*, and *UME1* as suppressors of phenotypes induced by high levels of D-2-HG. Rpd3 is a histone deacetylase, Sin3 and Ume1 are components of the Rpd3 histone deacetylase complex. The results suggest that histone deacetylase inhibitors (HDACi) might be an effective treatment for cancers comprising IDH mutations.

Kurzfassung

Der genetische Code allein ist nicht in der Lage die Vielfalt zellulärer und individueller Phänotypen zu erklären. Epigenetik liefert eine zusätzliche Informationsebene, welche nicht in der DNA kodiert ist, aber deren Aktivität trotzdem stabil und in vererbbarer Art und Weise beeinflusst. Epigenetische Regulation spielt eine entscheidende Rolle in der Onkogenese und die reversible Charakteristik dieser Abberationen führte zum Aufkommen der vielversprechenden epigenetischen Therapie.

Mutationen in NADP⁺ abhängigen Isocitrat-Dehydrogenasen (*IDH1* und *IDH2*) treten in vielen verschiedenen humanen malignen Tumoren auf. Dabei ist das Enzym nicht mehr in der Lage Isocitrat in α -Ketoglutarat umzuwandeln und es kommt stattdessen zur Akkumulation von D-2-HG in den Zellen. Dieser Onkometabolit inhibiert sowohl die Familie der TET DNA-DeMthylasen als auch jene der Jumonji Histondemethylasen. Die Folge sind epigenetischen Alterationen welche die Genexpression beeinflussen. Nichtsdestotrotz ist D-2-HG ein normaler endogener Metabolit welcher in allen Körperflüssigkeiten vorkommt und durch die Aktivität von D-2-Hydroxyglutarat Dehydrogenase (D2HGDH) in niedriger Konzentration aufrechterhalten bleibt. Die eigentliche Rolle dieses Metaboliten in der Zelle wurde bis dato noch nicht erforscht. Es ist daher von grösster Wichtigkeit mehr über die Aktivität von D-2-HG herauszufinden um in Zukunft effective Therapien fuer maligne Tumore welche IDH Mutationen aufweisen zu entwickeln.

Um dieser Forschungsaufgabe nachzugehen wurde ein Suppressor Screen in *S. cerevisiae* durchgeführt. Hierfür wurden Kulturen mit einer Mutation in der D-Laktat Dehydrogenase2 (Dld2) und Dld3 eingesetzt. Diese Enzyme sind die Hefeorthologe der humanen D-2-Hydroxyglutarate Dehydrogenase (D2HGDH), wodurch die Zellen folglich D-2-HG akkumulieren. Es wurde gezeigt, dass das Wachstum von Zellen mit der besagten Mutation durch Ethanol inhibiert wird. Drei verschiedene Suppressoren wurden im Screen gefunden, analysiert und sequenziert. Die Ergebnisse zeigen Mutationen in *RPD3*, *SIN3* und *UME1*. Rpd3 ist eine Histondeacetylase und Sin3 bzw. Ume1 sind Komponenten des Rpd3 deacetylase Komplexes. Diese Ergebnisse deuten darauf hin, dass Histon-Deacetylase-Inhibitoren (HDACi) eine effective Therapie für Krebszellen welche IDH Mutationen aufweisen sein könnten.

Contents

1	Introduction.....	8
1.1	What is Epigenetics.....	8
1.2	Epigenetics and silencing in yeast	11
1.3	Epigenetics, Metabolism and Cancer.....	12
1.4	The oncometabolite D-2-hydroxyglutarate (D-2-HG) and its role in cancer development	12
1.5	Goals of this work.....	13
2	Materials and Methods.....	14
2.1	Yeast strains	14
2.2	Suppressor screen.....	14
2.3	Whole genome sequencing and data analysis	15
2.4	Immuno-blotting	16
2.5	CRASH Assay	16
2.6	Flow Cytometry	17
3	Results.....	20
3.1	D-2-HG induces ethanol sensitivity	20
3.2	One mutated gene in each candidate found in the screen is responsible for suppression phenotype.....	21
3.3	Suppressor mutations were dominant	22
3.4	<i>set2Δ</i> phenocopied the suppression phenotype but sequencing showed no mutation in <i>SET2</i> ...	23
3.5	Whole genome sequencing identified point mutations in <i>RPD3</i> , <i>UME1</i> and <i>SIN3</i> being responsible for the suppression phenotype	23
3.6	The impact of D-2-HG on histone acetylation.....	24
3.7	Lower switching rate in <i>rpd3Δ</i> strains compared to wild type measured in flow cytometry.....	25
4	Discussion and Outlook	26
5	List of Figures	28
6	List of Tables	28
7	Bibliography	29

Acknowledgements

First of all, I would like to thank Prof. Jasper Rine for his great support and amazing leadership at UC Berkeley. Jasper definitely knows how to create a strong team and keep people motivated and excited.

I consider myself the luckiest person in the world having been able to do science in the Rine Lab. My co-worker and mentor Dr. Ryan Janke, who later also became a good friend is a phenomenon to me. I have never experienced a situation where he did not have time for immediately discussing results or just some simple questions. Thanks, Ryan, for all your patience and time you spent teaching me how to do science. Your mentorship stands out as a perfect example which I am hoping to be able to apply later in my career.

I would have definitely not made it through the past year without all the Rine Lab members. The high-spirited and fun Rine-os gave me the strength to come to lab even during difficult times. Thanks Katie, Davis, Gavin, Daniel, Marc, Jean, Victoria and Eliana for creating such a great environment at work. I will always cherish my memories of “funch”, coffee breaks, camping trips, sailing and the trip to Napa Valley.

I would also like to thank Prof. Kai-Uwe Fröhlich for his encouragement and for believing in me and my vision to be able to create proper results for my thesis.

I also have had such great family support over the past years. Even though my parents have a different background, they encouraged me during every step of the way and gave me the self-confidence I needed to succeed in school.

Words could never adequately express the amount of gratitude and love I have for my partner and best friend, Armin. His love, support, and encouragement gave me the strength to keep moving forward even in difficult times.

Finally, I would like to thank the Marshall Plan Foundation for their support. This endeavor would have not been possible without their generous funding.

1 Introduction

1.1 What is Epigenetics

The genetic code alone does not account for the entire range of phenotypes observed in nature. Epigenetics provides an additional layer of information that is not encoded in the DNA molecule but nonetheless influences its activity in a stable and heritable manner through cell division. Epigenetic regulation can convert a developmental or transient environmental signal into a stable transcriptional response and explains how, starting from a unique genome, the pluripotent embryo can generate a variety of tissues and maintain their identity throughout development (Bourc'his D, 2010). Epigenetic modifications can change recruitment of transcription factors, accessibility of the DNA to the transcriptional machinery, and alter the way the transcriptional machinery travels along a gene. Three epigenetic mechanisms present in human cells are described below.

- 1) **DNA methylation** (see Figure 1) plays an important role in genomic imprinting, inactivation of X-chromosome in females, maintaining the stability of the genome, regulation of transcription and also in the developmental process of an organism (Robertson KD, Jones PA, 2000). Methylated DNA is present in repetitive genomic regions (micro and mini-satellites), telomeres, within centromeres and parasitic elements such as short interspersed transposable elements (SINEs) and long interspersed transposable elements (LINEs) where they function to silence genes and non-coding genomic regions. The majority of DNA methylation occurring on cytosine residue is present in the CpG dinucleotide distributed throughout the genome and is also densely found in regions known as CpG islands (Jones PA, Takai D, 2001). In normal cells, the promoter regions of genes, especially those preceded by CpG islands are usually unmethylated, allowing transcription factors and other associated proteins to interact with the gene and facilitate their expression (Subhankar Biswas, C. Mallikarjuna Rao, 2017).

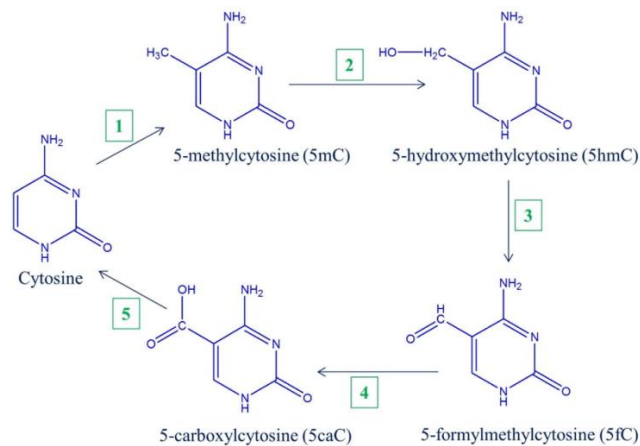


Figure 1: Modification of cytosine residue. The enzyme DNA methyltransferase methylates cytosine residue present in DNA at C5 position to form 5mC (1). TET1-3 enzymes then oxidize 5mC (2) to form 5hmC. Over-activity of TET enzymes (3,4) can further oxidize 5hmC into 5fC and 5caC. The enzyme Thymine-DNA glycosylase (5) removes the carboxyl group from 5caC following which base excision repair pathway (5) converts it into unmodified cytosine (Subhankar Biswas, C. Mallikarjuna Rao, 2017).

- 2) **Histone modifications:** The basic element of chromatin, the nucleosome core particle, wraps 147 base pair of DNA around an octamer of four core histone proteins, see Figure 2. The basic histone proteins comprise an inherent positive charge which provides efficient binding with negatively charged DNA. The four core histones are present as two H2A-H2B dimers and an H3-H4 tetramer in association with a linker histone H1, which joins nucleosomes together. The sequence of amino acids comprising the histone proteins vary substantially among different species. But the histone proteins are made up of a common structural domain called the “histone fold”. These folds comprise of a long central helix linked with two helix-strand-helix motifs at the opposite ends (Subhankar Biswas, C. Mallikarjuna Rao, 2017). The N-terminal tails of histones are highly flexible and are rich in lysine and arginine residues which can be extensively modified by a large number of cellular systems (Ramakrishnan V, 1997). Posttranslational, covalent modifications on those tails include methylation, acetylation, ubiquitination, sumoylation and phosphorylation on specific residues (Shikhar Sharma, Theresa K. Kelly, and Peter A. Jones, 2009). Acetylation of histone tail lysine residues is associated with transcriptionally active chromatin. Acetylation removes the net positive charge on the histone proteins by acetylating the ϵ -amino group of lysine residues using acetyltransferases (HATs) which utilizes acetyl-CoA as the acetyl group donor (Subhankar Biswas, C. Mallikarjuna Rao, 2017).

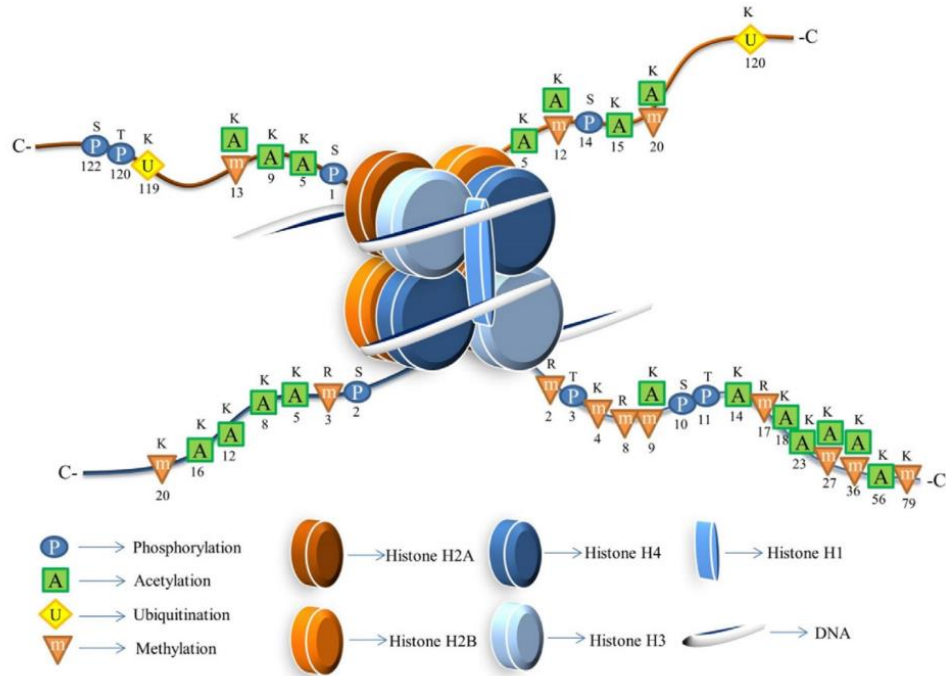


Figure 2: Histone modifications. The basic unit of DNA packaging in eukaryotes are nucleosomes. Each particle consists of an octamer of histone proteins including H2A, H2B, H3 and H4. Histones comprise N-terminal tails which play an important role in modulating nucleosome structure and function. Modifications on the different residues of histone tails are being shown here. S, T, K and R represent Serine, Threonine, Lysine and Arginine respectively. (Subhankar Biswas, C. Mallikarjuna Rao, 2017).

- 3) **MicroRNAs (miRNAs)** are small non-coding RNAs which are endogenous molecules and around 16 to 22 nucleotides long. Transcription of miRNAs is carried out by the enzyme RNA polymerase II to form the primary microRNA (pri-miRNA), which is processed by the microprocessor complex (DROSHA and DGCR8) to generate the precursor miRNA (pre-miRNA). The pre-miRNA is exported into the cytoplasm by Exportin 5 in association with Ran-GTP. The pre-miRNA is further processed by DICER in the cytoplasm to generate a double stranded RNA. The double stranded RNA cleaves to form a mature miRNA, which associates with RNA induced silencing complex (RISC). The mature miRNA guides RISC to recognize the target mRNA leading to mRNA degradation or translation repression (Figure 3) (Subhankar Biswas, C. Mallikarjuna Rao, 2017) (Garzon R, Fabbri M, Cimmino A, Calin GA, Croce CM., 2006).

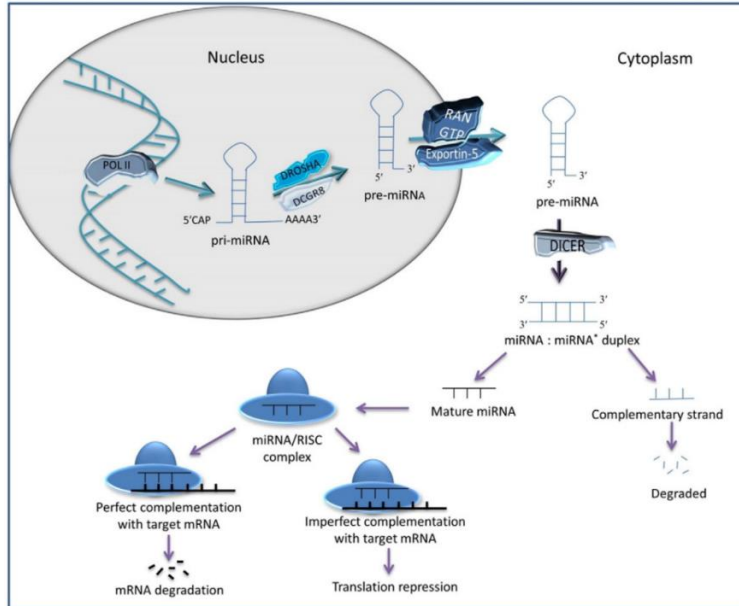


Figure 3: miRNA biogenesis. (Subhankar Biswas, C. Mallikarjuna Rao, 2017). For detailed description see text above.

1.2 Epigenetics and silencing in yeast

Genetic and biochemical studies using yeast have been extremely fruitful in illuminating many epigenetic modifications and their impacts, most of which have proven to be widely conserved. Gene silencing in *Saccharomyces* occurs in part by an epigenetic mechanism resulting from the assembly of heterochromatin at the loci to be silenced (Grunstein M, Gasser SM., 2013). The structural proteins of heterochromatin in *Saccharomyces* are the Silent Information Regulatory (SIR) proteins Sir1, Sir2, Sir3 and Sir4 (Rine J, Herskowitz I., 1987). Silencing in *Saccharomyces* occurs by the recruitment of a complex of Sir2, Sir3 and Sir4 to regulatory sites called silencers, aided by the Sir1 protein bound to silencers. The Sir complex then deacetylates H4K16-acetyl (H4K16-Ac) on neighboring nucleosomes, and such deacetylated H4 tails provide binding sites for additional Sir-protein complexes (Hecht A, Laroche T, Strahl-Bolsinger S, Gasser SM, Grunstein M., 1995). After rounds of deacetylation and binding of additional Sir-protein complexes, silenced domains of chromatin consist of hypoacetylated nucleosomes bound continuously by Sir-protein complexes, see Figure 4 below (Ellahi A, Thurtle DM, Rine J., 2015) (Thurtle DM, Rine J., 2014). Chromatin with this molecular topography blocks access of other site-specific DNA binding proteins to their cognate binding sites (Loo S, Rine J., 1994) (Steakley DL, Rine J, 2015). Humans possess seven siruin paralogs implicated in a rich variety of diseases including cancer (Imai S, Guarente L, 2014).

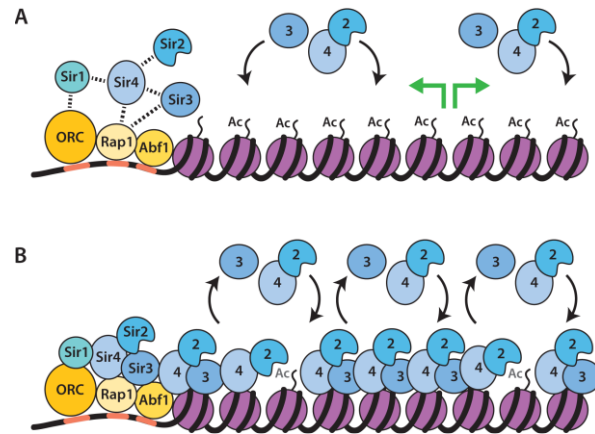


Figure 4: Establishment and maintenance of silencing. (Anne E. Dodson, 2016) A- Establishment of silencing. Silencer binding proteins (ORC, Rap1, Abf1) recruit the sir proteins (sir1, sir2, sir3, sir4). Dashed lines indicate direct interactions. When sir proteins are assembled at the silencers more sir proteins get recruited to the locus to be silenced. First sir2 deacetylates H4K16 acetyl mark, then sir3 and sir4 bind to nucleosomes. B- Sir2 mediated deacetylation and recruitment of more sir protein continuously reinforces the silenced state.

1.3 Epigenetics, Metabolism and Cancer

Cancer metabolism is one of the oldest areas of research in cancer biology. Metabolic activities are altered in cancer cells relative to normal cells. These alterations support the acquisition and maintenance of malignant properties. Some altered metabolic features are observed quite generally across many types of cancer cells and reprogrammed metabolism is therefore considered a hallmark of cancer. Changes in metabolite levels can affect cellular signaling, epigenetics, and gene expression through posttranslational modifications such as acetylation and methylation (Ralph J. DeBerardinis and Navdeep S. Chandel, 2016). This was also confirmed by other members of the UC Berkeleys Rine Lab like Dr. Ryan Janke. He found out recently that the oncometabolite D-2-hydroxyglutarate (D-2-HG) enhances gene silencing through inhibition of specific H3K36 histone demethylase in yeast (Ryan Janke, Anthony T Iavarone, Jasper Rine, 2017).

1.4 The oncometabolite D-2-hydroxyglutarate (D-2-HG) and its role in cancer development

Cancer-associated *IDH1* and *IDH2* mutations result in a gain of function in which α -ketoglutarate (α -KG) is reduced to produce D-2-HG, (Figure 5) (Shenghong Ma et al., 2015). α -KG plays crucial roles in the

TCA-cycle, amino acid synthesis and nitrogen transport (Ryan Janke, Anne E. Dodson, Jasper Rine, 2015). D-2-HG inhibits α -KG dependent dioxygenases, including TET DNA demethylases and Jumonji histone demethylases, resulting in widespread changes in DNA and histone methylation patterns and gene expression (Ryan Janke, Anthony T Iavarone, Jasper Rine, 2017). Figure 5 shows in which metabolic pathways D-2-HG is involved in.

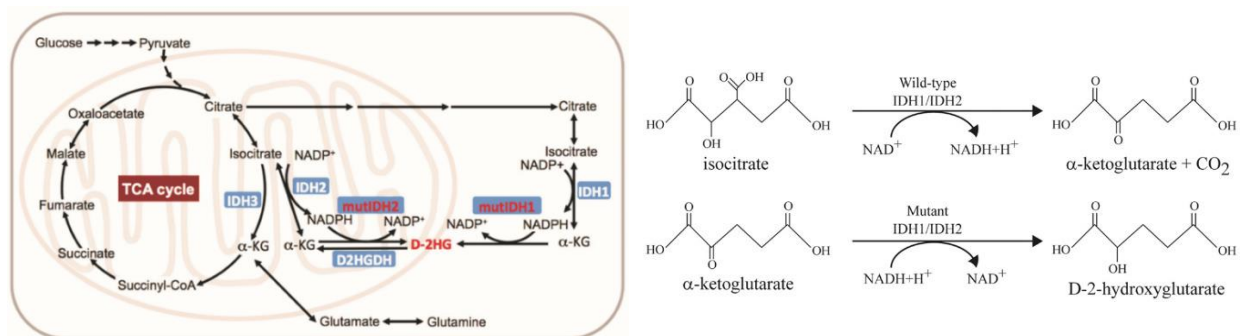


Figure 5: Scheme of metabolic pathways involved in D-2-HG metabolism and enzymatic reactions catalyzed by wild-type and mutant IDH enzymes. α -KG is a key intermediate in the TCA cycle for energy metabolism and also acts as an entry point for amino acids to enter the TCA cycle (Shenghong Ma et al., 2015). Mutated IDH1 and IDH2 reduce α -ketoglutarate to D2HG while converting NADH and H⁺ to NAD⁺ (Nadine F. Voelxen et al., 2016).

1.5 Goals of this work

D-2-HG accumulates in various types of cancers such as, gliomas, secondary glioblastomas, acute myelogenous leukemia, cholangiocarcinoma, cartilaginous tumors, prostate cancer, papillary breast carcinoma, acute lymphoblastic leukemia, angioimmunoblastic T-cell lymphoma, and primary myelofibrosis. This indicates that D-2-HG is an important player in multiple types of cancers (Adam Cohen, Sheri Holmen, and Howard Colman, 2013). Fundamental understanding of the function of this metabolite in cells and the mechanisms behind it, is still lacking. The primary goal of this work was to understand the impact of D-2-HG on cells and the mechanisms that underlie the effect on cell physiology. Identifying genes that interact with high levels of D-2-HG will provide insight into the physiological role of this metabolite in cells. Therefore, performing a suppressor screen was the first logical step towards being able to combat a variety of malignant tumors in the future.

2 Materials and Methods

2.1 Yeast strains

The strains and oligonucleotides used in this study are listed in Table 1 and Table 2, respectively at the end of this chapter. All strains were derived from the W303 background. Deletions were made using one-step integration of gene disruption cassettes and confirmed by PCR. This process is described in more detail in the following references (Longtine MS1, McKenzie A 3rd, Demarini DJ, Shah NG, Wach A, Brachat A, Philippsen P, Pringle JR., 1998), (Goldstein AL, McCusker JH., 1999), (Wach A, Brachat A, Pöhlmann R, Philippsen P, 1994).

2.2 Suppressor screen

A suppressor screen (as shown in Figure 6) was used to identify suppressor mutations which alleviate or revert the phenotype of the original mutation(s) (in this study *dld2Δdld3Δ*). Suppressor mutations occur as secondary mutations at sites distinct from the mutation under study, which suppresses the phenotypic effect of the original mutant (Jonathan Hodgkin, 2005). Suppressor mutations help define relationships between different biochemical pathways (Fabio Puddu, Tobias Oelschlaegel et al., 2015).

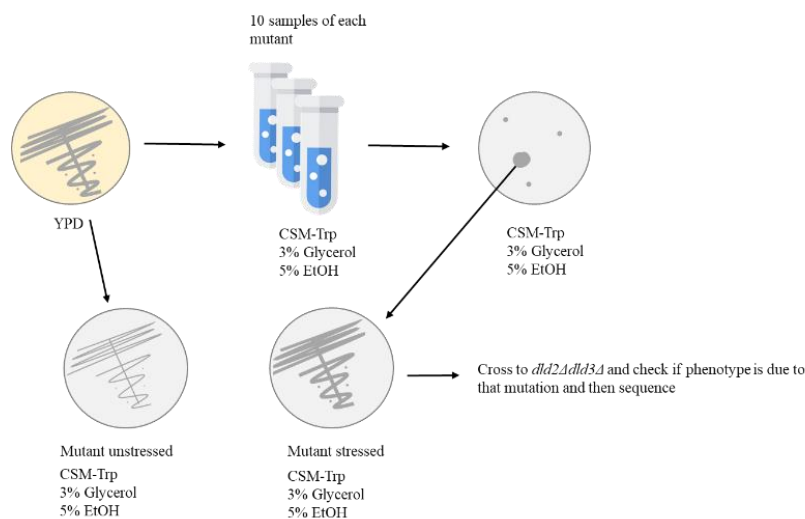


Figure 6: Schematics showing the procedure of the suppressor screen. Description can be found in text below.

Procedure of the screen

Ten single colonies of each mutant (*dld2Δ*, *dld3Δ*, *dld2Δdld3Δ*) were grown until saturation in CSM-Trp 3% Glycerol 5% EtOH liquid media and plated with different dilutions on CSM-Trp glycerol 5% EtOH plates. The plates were incubated at 30°C for 5 days until colonies formed. Large colonies were selected and verified for increased resistance to ethanol by plating serial dilutions of each strain onto media containing 3% and 5% ethanol.

To determine if suppressor phenotypes were monogenic in nature, suppressor candidates were backcrossed to the original *dld2Δdld3Δ* mutant strain and segregation of the phenotype was documented. Complementation tests were performed to determine whether the various suppressor mutations identified were due to mutations in the same or different loci.

Dominance of the suppressor alleles was carried out by mating haploid candidate strains to the original haploid *dld2Δdld3Δ* mutant to generate diploids which were tested for sensitivity to ethanol.

2.3 Whole genome sequencing and data analysis

DNA for whole-genome sequencing analysis was isolated following the yeast DNA extraction protocol in (Charles S.Hoffman, Fred Winston, 1987).

The data received from the UC Berkeley Vincent J. Coates Genomics Sequencing Laboratory (GSL) were 100bp paired end. Each sample was mapped to the SacCer3 reference genome using data available at *yeastgenome.org* and the mapping results were sorted according to their position along the genome.

Then, a command called *mpileup* that generates a table of all sites in the genome, and scores how often they are counted, or how often there is a mutation at that position was generated. The generated file was fed into a program called *bftools*, which identified sites that have real mutations (rather than sequencing errors). A separate list of sites that have mutations for each mutant pool and for the wild-type pool was made, then a custom code in the programming language *R* was written by Gavin Schlissel to compare them and identify the mutations that are present in the "suppressed" pools but not in the wild-type pools. In the last step, those mutations were fed into a program called *SnEff*, and *SnEff* returned the genes in which each mutation occurs, and a prediction for how severe the mutation was.

2.4 Immuno-blotting

Immunoblots were performed as described in the following reference (Ryan Janke, Anthony T Iavarone, Jasper Rine, 2017). Cells were grown in liquid cultures of CSM-Trp-3% glycerol shaking at 30°C until mid-log phase. Ten OD units of cells were harvested from each culture, pelleted, frozen with liquid nitrogen, and stored at -80°C. Pellets were resuspended in 200 µl of 20% w/v trichloroacetic acid and transferred to 2-ml screw cap tubes. Cell extracts were prepared by addition of an equal volume of 0.5 mm zirconium ceramic beads (*BioSpec Products*, Bartlesville, OK) followed by bead beating using a *Millipore MP-20 FastPrep* (*EMD Millipore*, Billerica, MA) on setting 5.5 with 20 s cycle duration. A total of five cycles were performed with 2-min incubations on ice between each run to prevent overheating of samples. Recovered precipitate was dissolved in 200 µl of 2X *Laemmli* buffer and the pH adjusted by adding 30 µl of 1.5 M Tris pH = 8.8. Samples were heated at 65°C for 10 min and insoluble material was pelleted by centrifugation. An equal amount of the soluble portion of each sample was run on SDS-polyacrylamide gels and transferred to nitrocellulose membranes. Membranes were blocked in Li-Cor Odyssey Blocking Buffer (*LI-CORE Biosciences*, Lincoln, NE) and the following primary antibodies were used for immunodetection: anti-acetyl histone H4 (Lys12) polyclonal antibody was from *Millipore*, anti-phosphoglycerate kinase antibody (22C5D8) from *ThermoFisher* (Rockford, IL.). Membranes were incubated with infrared dye-conjugated secondary antibodies, IRDye800CW goat anti-mouse and IRDye680RD goat anti-rabbit antibodies (*LI-CORE Biosciences*, Lincoln, NE) and imaged on a *LI-CORE Odyssey* imager in the 700 nm and 800 nm channels. All washing steps were performed with Tris-buffered saline – 0.05% Tween-20. Quantitative analysis of immunoblots was performed using *LI-CORE Image Studio* software (*LI-CORE Biosciences*, Lincoln, NE).

2.5 CRASH Assay

The CRASH assay (Cre-Recombinase Assessment of Stability of Heterochromatin), involves the Cre-recombinase placed under the control of a promoter silenced by heterochromatin at the *HML* locus. A cassette consisting of red fluorescent protein (RFP) expressed by a constitutive yeast promoter, and a promoterless gene encoding green fluorescent protein (GFP) downstream of the RFP gene was inserted at the *URA3* locus. Lox sites, at which the Cre-recombinase can act, were positioned such that if Cre was expressed, the RFP coding sequence was looped out of the chromosome, permanently fusing the GFP gene

to the constitutive promoter, as shown in Figure 7 (Anne E Dodson, Jasper Rine, 2015). Thus, transient losses of silencing resulted in a switch of a red cell and all its descendants into green cells. Therefore, the number and size of sectors reflected epigenetic stability. Loss-of-silencing events at *HML* occurs in 1.6×10^{-3} cell divisions. This rate also allows for advanced microscopic and flow cytometry applications to interrogate the molecular events in these cells with single-cell resolution (Anne E Dodson, Jasper Rine, 2015).

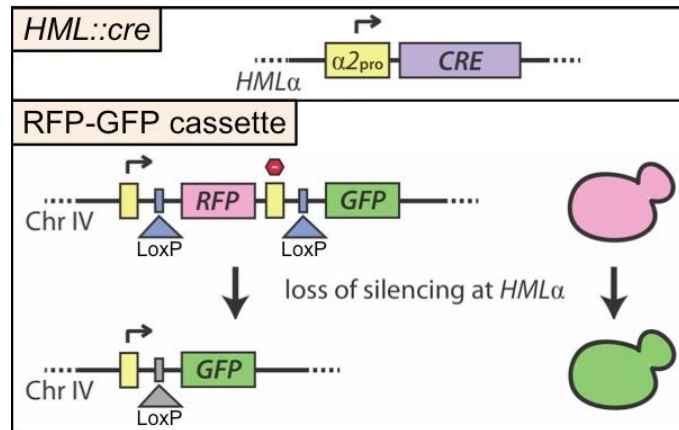


Figure 7: Schematics of CRASH-Assay (Anne E Dodson, Jasper Rine, 2015)

2.6 Flow Cytometry

Quantification of Silencing Loss by Flow Cytometry

For each CRASH strain, ten single colonies were inoculated separately into 1 ml of CSM-Trp 3% Glycerol media in 96-deep-well plates and grown overnight to saturation at 30°C on a low orbital shaker. Overnight cultures were diluted into 1 ml of fresh media at a density of 10⁵ cells/ml in 96-deep-well plates and were grown at 30°C on a low orbital shaker until mid-log phase. For each culture, a minimum of 50,000 events were collected using an *Attune NxT Flow Cytometer* (by Life Technologies). Scatterplots of forward scatter (height) and forward scatter (width) measurements were generated and gating was established to include only singlets (unbudded) and budded cells and exclude debris as well as clumped cells for further analysis. Gating was used to separately measure the number of GFP-positive cells and the number of RFP-positive cells. Finally, a *Boolean logic gate* ‘RFP+ AND GFP+’ was used to determine the number of cells that were both GFP and RFP fluorescent. Such cells were inferred to have just undergone the Cre-mediated

recombination event leading to GFP expression, yet retained RFP expressed in the recent past. The frequency of switching was calculated by dividing the number of cells in a population that had very recently lost silencing (cells that are both GFP- and RFP-fluorescent) by the number of cells in the population that had the potential to lose silencing (cells that are only RFP-fluorescent + cells that are both GFP- and RFP-fluorescent). Boxplots were generated where the median value was calculated from at least 10 cultures. The boxes in Figure 16 represent the 25th and 75th percentile. Whiskers represent the range of values within 1.5-times the interquartile range. Unpaired two-sided (Student's) t tests were used to determine whether differences in frequency of silencing loss were statistically significant.

Table 1: Strains used in this study. All strains are so called “CRASH strains”. A more detailed description can be found in section 2.5 or in the following publication (Dodson A, Rine J, 2015).

Strain	Genotype
RHJY42	<i>MATα</i> ADE2, <i>lys2</i> , <i>TRP1</i> , <i>hmlα2Δ::CRE</i> , <i>ura3Δ::pGPD:loxP:yEmRFP;tCYC1:Hygmx:loxP:yEGFP:tADH1 dld2Δ::URA3</i> (<i>C. albicans</i>)
RHJY43	<i>MATα</i> ADE2, <i>lys2</i> , <i>TRP1</i> , <i>hmlα2Δ::CRE</i> , <i>ura3Δ::pGPD:loxP:yEmRFP;tCYC1:KanMX:loxP:yEGFP:tADH1 dld2Δ::URA3</i> (<i>C. albicans</i>)
RHJY63	<i>MATα</i> ADE2, <i>lys2</i> , <i>TRP1</i> , <i>hmlα2Δ::CRE</i> , <i>ura3Δ::pGPD:loxP:yEmRFP;tCYC1:hygMX:loxP:yEGFP:tADH1</i>
RHJY65	<i>MATα</i> ADE2, <i>lys2</i> , <i>TRP1</i> , <i>hmlα2Δ::CRE</i> , <i>ura3Δ::pGPD:loxP:yEmRFP;tCYC1:hygMX:loxP:yEGFP:tADH1</i>
RHJY165	<i>MATα</i> ADE2, <i>lys2</i> , <i>TRP1</i> , <i>hmlα2Δ::CRE</i> , <i>ura3Δ::pGPD:loxP:yEmRFP;tCYC1:hygMX:loxP:yEGFP:tADH1 dld3Δ::kanmx dld2Δ::URA3</i> (<i>C. albicans</i>)
RHJY212	<i>MATα</i> ADE2, <i>lys2</i> , <i>TRP1</i> , <i>hmlα2Δ::CRE</i> , <i>ura3Δ::pGPD:loxP:yEmRFP;tCYC1:hygMX:loxP:yEGFP:tADH1 dld2Δ::URA3</i> (<i>C. albicans</i>) <i>dld3Δ::KANMX</i>
RHJY297	<i>MATα</i> ADE2, <i>lys2</i> , <i>TRP1</i> , <i>hmlα2Δ::CRE</i> , <i>ura3Δ::pGPD:loxP:yEmRFP;tCYC1:hygMX:loxP:yEGFP:tADH1 dld3Δ::kanmx dld2Δ::URA3</i> (<i>C. albicans</i>) <i>rdp3Δ::natMX</i>
RHJY296	<i>MATα</i> ADE2, <i>lys2</i> , <i>TRP1</i> , <i>hmlα2Δ::CRE</i> , <i>ura3Δ::pGPD:loxP:yEmRFP;tCYC1:hygMX:loxP:yEGFP:tADH1 rdp3Δ::natMX</i>

Table 2: Oligonucleotides used in this study.

Oligonucleotide	Sequence (5'-3')
RPD3 KO For	TACAAAACATTCGTGGCTACAACCTCGATATCCGTGCAGGCATAGGCCACTA GTGGATCT
RPD3 KO Rev	TCACATTATTTATATTCGTATATACTTCCAACCTCTTTTTTCAGCTGAAGCTT CGTACGC
RPD3 co For	AAGTAATATCAACTCAGAGCGTATAGGTAAATTTGTAAAT
RPD3 co Rev	GTTTAGATAGTAATTACAATAGAAATACAACCTGTTTCAAT

3 Results

3.1 D-2-HG induces ethanol sensitivity

The mutants under investigation (*dld2Δ*, *dld3Δ*, *dld2Δdld3Δ*) have never been subject of a suppressor screen. Therefore, different carbon sources and then different stresses were tested, see Table 3.

Table 3: Carbon sources and stresses tested in the suppressor screen.

Carbon sources	Stresses
- Glucose	- H ₂ O ₂
- Raffinose	- Sorbitol
- Galactose	- Hydroxyurea
- Glycerol	- Ethanol

The strains turned out to be sensitive to EtOH as can be seen in Figure 8.

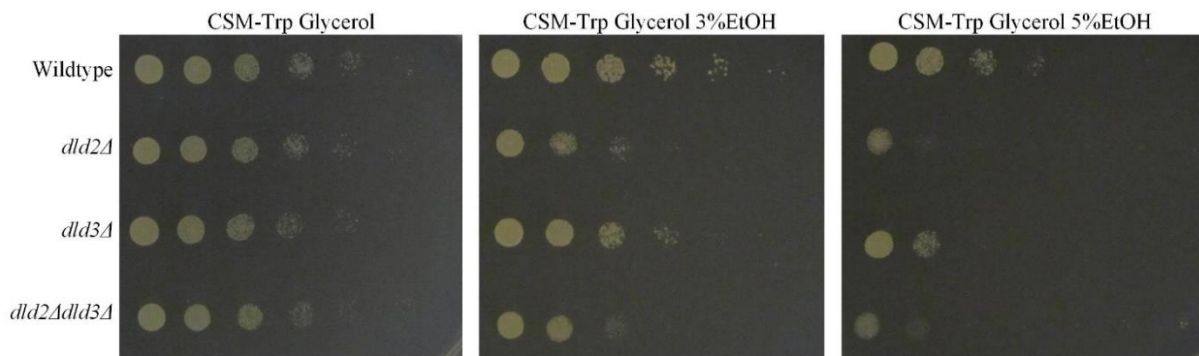


Figure 8: Sensitizing conditions found. Fivefold serial dilutions of yeast were spotted on plates to determine their growth phenotype. Plated on CSM-Trp 3% Glycerol for the control and 3% or 5% EtOH added to the media to check for a difference in growth. All the strains are *MATa*.

Performing the screen as described in the method section, three suppressors were found. All of them in the *dld2Δdld3Δ* background. Candidates are shown in Figure 9 below.

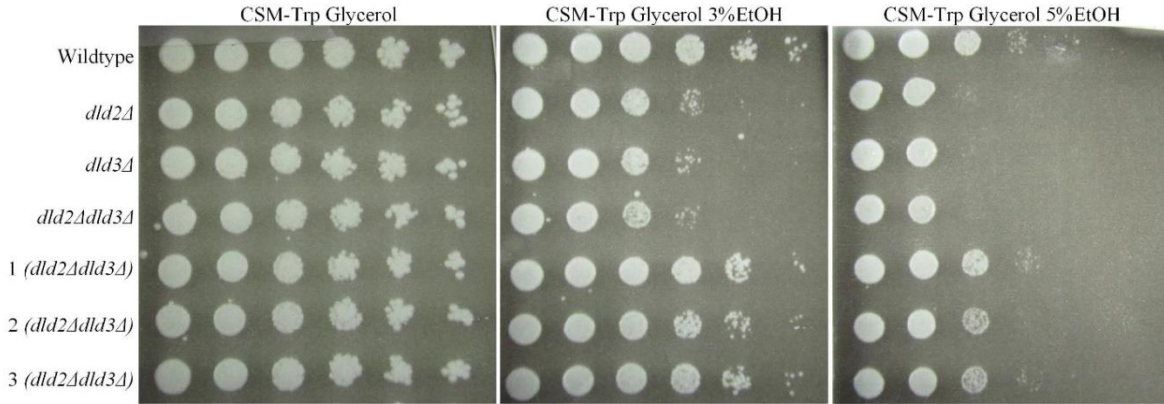


Figure 9: Suppressors found. Fivefold serial dilutions of yeast were spotted on plates to determine their growth phenotype. Number 1-3 with a *dld2Δdld3Δ* background are the 3 candidates found in the suppressor screen. All strains are *MATa*.

3.2 One mutated gene in each candidate found in the screen is responsible for suppression phenotype

After having found three candidates, which suppress the growth phenotype of ethanol sensitivity, the next step was to determine whether a single locus was responsible for that phenotype. Therefore, the suppressor candidates were mated back to the original mutant strain (*MATα dld2Δdld3Δ*), sporulated and the resulting tetrads were dissected. Two tetrads of each candidate were tested by drop-dilution assay. The suppressor phenotype showed a segregation pattern of 2:2. One typical example is displayed in Figure 10.

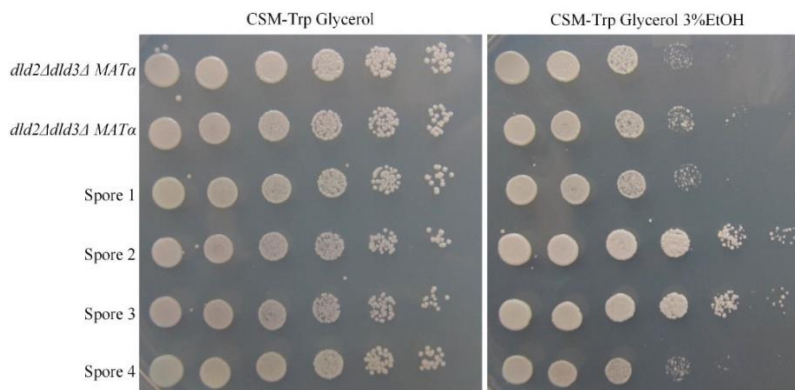


Figure 10: One mutated gene responsible for growth phenotype. Fivefold serial dilutions of yeast were spotted on plates to determine their growth phenotype. Suppressor candidate with a *dld2Δdld3Δ* background was mated to *MATα dld2Δdld3Δ* and dissected. The first two rows show the controls *MATa* and *MATα* respectively. Row 3-6 display the dissected spores.

A complementation test was performed to determine whether the mutations in the suppressor candidates were in the same complementation group. The suppressor mutant strains were mated to each other (1x2, 1x3, 2x3) and the resulting diploid strains were spotted on plates containing EtOH of different concentrations. Figure 11 shows that the growth phenotype of the suppressors match the *dld2Δdld3Δ* diploid and not wild type.

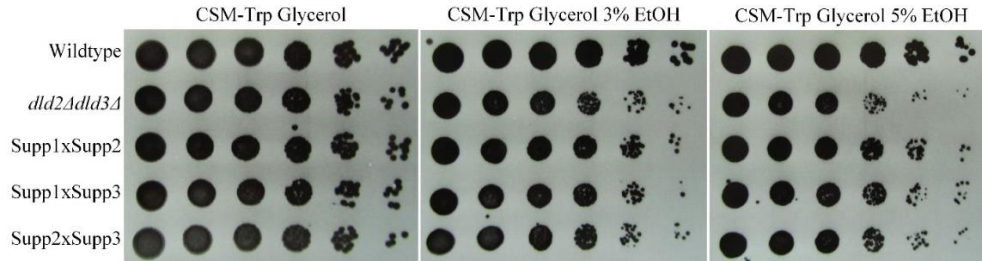


Figure 11: Complementation assay. Fivefold serial dilutions of yeast were spotted on plates to determine their growth phenotype. All strains displayed are diploids. Row 1 and 2 are the controls wild type and *dld2Δdld3Δ*, respectively. Row number 3 shows the diploid consisting of suppressor candidate no 1 and no 2. The diploid in row 4 displays candidate no 1 and 3 and in the last row no 2 was mated to no 3.

3.3 Suppressor mutations were dominant

To find out whether the suppressor phenotypes were dominant or recessive, three haploid suppressor candidates and the original mutant were mated to *MAT α dld2Δdld3Δ* and the resulting diploids were plated. Different growth phenotypes are displayed in Figure 12. All suppressor candidates showed less sensitivity to EtOH compared to the original mutant *dld2Δdld3Δ*.

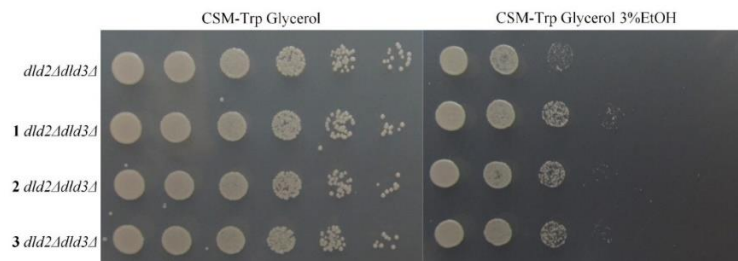


Figure 12: Test for dominance. Fivefold serial dilutions of yeast were spotted on plates indicated to determine their growth phenotype. Row 1 shows the original mutant *dld2Δdld3Δ*. Number 1-3 with a *dld2Δdld3Δ* background are the 3 candidates found in the suppressor screen. All the strains are diploids mated to *MAT α dld2Δdld3Δ*.

3.4 *set2Δ* phenocopied the suppression phenotype but sequencing showed no mutation in *SET2*

H3K36 methylation levels increase in a *dld2Δ*, *dld3Δ* or *dld2Δdld3Δ* strain (Ryan Janke, Anthony T Iavarone, Jasper Rine, 2017). Set2 is the only methyltransferase for H3K36 methylation in budding yeast. To check whether the growth phenotype seen in the suppressors was due to a mutation in *SET2*, *SET2* was deleted and a drop assay was performed on media indicated in Figure 13. In the drop assay it is shown that a *dld2Δset2Δ* mutant led to the exact same growth phenotype. Nevertheless, results from sequencing did not show a mutation in the *SET2* gene in any of the suppressor candidates. That means that ethanol sensitivity was due to H3K36 hypermethylation but suppression of that sensitivity was not due to a mutation in *SET2*.

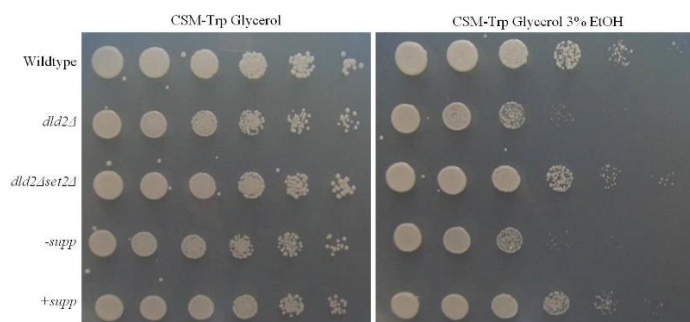


Figure 13: Deletion of *SET2* in a *dld2Δ* background phenocopies suppression phenotype. Fivefold serial dilutions were spotted on indicated media to determine growth phenotype. All strains are *MATa*. The first two rows display the control wild type and *dld2Δ*. The third row shows the *dld2Δset2Δ* double mutant. Row number 3 and 4 show the suppressor without the point mutation and suppressor with the point mutation respectively.

3.5 Whole genome sequencing identified point mutations in *RPD3*, *UME1* and *SIN3* being responsible for the suppression phenotype

After having analyzed the results from the UC Berkeley Vincent J. Coates Genomics Sequencing Laboratory (GSL) as described above in 2.3, the first candidate showed a point mutation in the *RPD3* gene. The second candidate showed a mutation in the *UME1* gene and the third suppressor candidate comprised a mutation in the *SIN3* gene. Rpd3 is a histone deacetylase responsible for the deacetylation of lysine residues on the N-terminal part of the core histones (H2A, H2B, H3 and H4). Ume1 and Sin3 are catalytic components of the Rpd3 histone deacetylase complex (Xiao-Fen Chen, Benjamin Kuryan et al., 2012). To confirm these results, knockouts were made starting with *rpm3Δ*. In Figure 14 it can be seen that *rpm3Δ*

looks like wildtype and that the triple mutant *dld2Δdld3Δrpd3Δ* clearly shows the suppression phenotype when compared to the *dld2Δdld3Δ* double mutant.

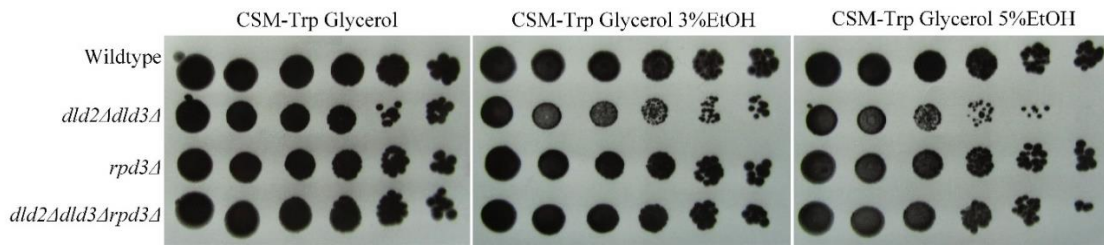


Figure 14: RPD3 deletion in a *dld2Δdld3Δ* mutant leads to suppression phenotype. Fivefold serial dilutions were spotted on indicated media to determine the growth phenotype. All strains are *MATa*. The first row shows wild type and the second one displays the *dld2Δdld3Δ* double mutant. Row number 3 and 4 show the *rpd3Δ* single mutant and *dld2Δdld3Δrpd3Δ* triple mutant respectively.

3.6 The impact of D-2-HG on histone acetylation

H4K5-acetyl, H4K8-acetyl, and H4K12-acetyl are the known substrates on H4 for Rpd3 in yeast nucleosomes (Deborah M. Thurtle-Schmidt, Anne E. Dodson, and Jasper Rine, 2016). Due to lack of time only H4K12 acetylation levels were tested in this work. In Figure 15 changes in acetylation are displayed in wild type, *dld2Δdld3Δ*, *rpd3Δ*, *dld2Δdld3Δrpd3Δ*, and the suppressor candidate found in the screen. H4K12 was hyperacetylated not only in the *dld2Δdld3Δrpd3Δ* triple mutant and the suppressor candidate, but also in the *rpd3Δ* single mutant compared to wild type. A difference in acetylation levels was not observed between wild type and the *dld2Δdld3Δ* double mutant.

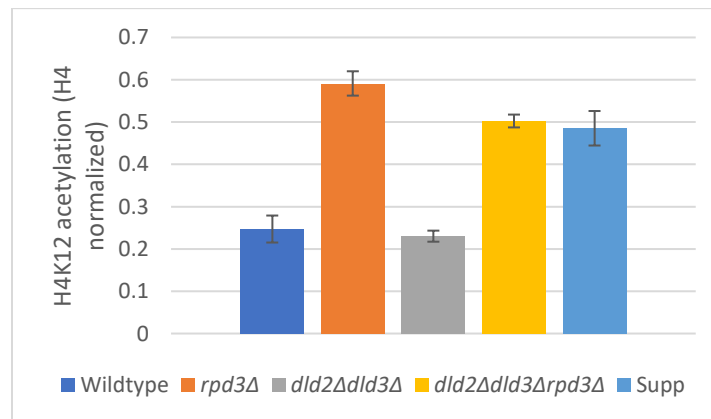


Figure 15: Acetylation levels of H4K12 in wild type, *dld2Δdld3Δ*, *rpd3Δ*, *dld2Δdld3Δrpd3Δ*, Suppressor candidate found in the screen. P-value between wild type and *rpd3Δ* is 0.0013, so significantly different. P-value between *rpd3Δ* and *dld2Δdld3Δ* is also 0.0013. Values are normalized to H4. Error bars are standard error of the mean.

3.7 Lower switching rate in *rpd3Δ* strains compared to wild type measured in flow cytometry

Histone acetylation, which should be increased when Rpd3 function is lost, is generally correlated with transcriptional activity. However, *RPD3* deletions result in increased genomic silencing (De Rubertis F, Kadosh D, Henchoz S, Pauli D, Reuter G, Struhl K, Spierer P, 1996). To check whether the additional mutation of *dld2Δdld3Δ* affects this phenotype, switching rates in flow cytometry were determined. In Figure 16 switching rates are displayed. It must be noted that wild type and *dld2Δdld3Δ* double mutant are statistically different. Furthermore, *dld2Δdld3Δrpd3Δ* and the suppressor (with a point mutation in *RPD3*) found in the screen, showed a significantly lower switching rate than *dld2Δdld3Δ* double and *rpd3Δ* single mutant.

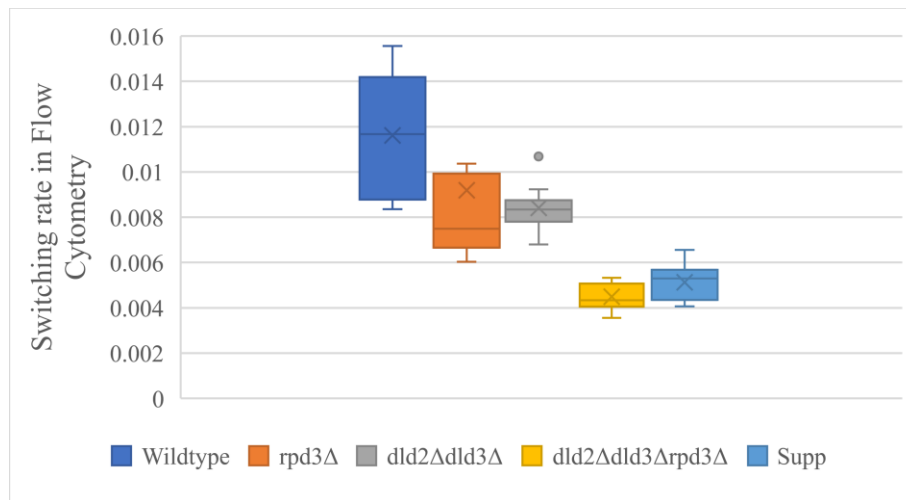


Figure 16: Flow Cytometry Error bars are standard error of the mean. P-value between *dld2Δdld3Δ* and *dld2Δdld3Δrpd3Δ* is less than 0.0001 and therefore the result is statistically significant. Wild type and *dld2Δdld3Δ* are also significantly different with a p-value of 0.0039. Unpaired two-sided (Student's) t tests were used to determine whether differences in frequency of silencing loss were statistically significant.

4 Discussion and Outlook

The oncometabolite D-2-HG accumulates in various types of cancers comprising *IDH1* or *IDH2* mutations. Fundamental understanding of the function of this metabolite in cells and the mechanisms behind it, is still lacking. In this study a suppressor screen was performed to identify genes that interact with high levels of D-2-HG to provide insight into the physiological role of this metabolite in cells.

Three suppressor candidates were found in this study. Experiments like the complementation assay, confirmed that mutations were not in the same complementation group meaning different mutations in every candidate were responsible for the suppression phenotype. Also, segregation patterns of 2:2 indicate that one gene in each suppressor was responsible for the growth phenotype. Sequencing results revealed point mutations in *RPD3*, *UME1*, and *SIN3*.

Strains that were heterozygous for the suppressor mutants showed suppression of ethanol sensitivity, suggesting either that the mutations are dominant or haploinsufficient. To distinguish between these two possible interpretations, a plasmid containing wild-type *RPD3* could be added back to haploid suppressor candidates. If a copy of wild type *RPD3* restored ethanol sensitivity in to the haploid suppressor strain, it would indicate that the suppressor mutant phenotype is recessive, and that the results in figure 12 are due to haploinsufficiency in the heterozygous diploid.

In the immunoblot, H4K12 acetylation levels were elevated when *RPD3* was mutated. No difference was detected between wild type and *dld2Δdld3Δ* double mutant. This might be due to the fact that a different acetylation site is responsible for the phenotype discovered. Different acetyl marks Rpd3 acts on need to be looked at and a Chip-seq experiment would be the next step forward.

In the flow cytometry experiment the switching rate in the *dld2Δdld3Δrpd3Δ* triple mutant was significantly lower than in *rpd3Δ* or *dld2Δdld3Δ* mutant alone. This indicated that the phenotypes might be additive. A *dld2Δdld3Δ* mutant accumulates D-2-HG leading to H3K36 hypermethylation and more stable heterochromatin (Ryan Janke, Anthony T Iavarone, Jasper Rine, 2017). As already known, Rpd3 counteracts genomic silencing. Rpd3 subunit gets recruited to H3K36 via the chromodomain of Eaf3, leading to deacetylation (Lee JS, Shilatifard A., 2007). In a *dld2Δdld3Δrpd3Δ* triple mutant, hypermethylation of H3K36 occurred but deacetylation of H3K12 via Rpd3 was not observed, leading to even more stable heterochromatin.

In the drop assays, mutations in *RPD3*, *SIN3* or *UME1* in combination with *dld2Δdld3Δ* mutations restored growth back to wild type levels. *SIN3* and *UME1* knockouts still need to be investigated but nevertheless this is an interesting observation, which raises the question whether HDACi might be an effective treatment in cancers comprising IDH mutations.

5 List of Figures

Figure 1: Modification of cytosine residue	9
Figure 2: Histone modifications.....	10
Figure 3: miRNA biogenesis	11
Figure 4: Establishment and maintenance of silencing.....	12
Figure 5: A scheme of metabolic pathways involved in D-2-HG metabolism and enzymatic reactions catalyzed by wild-type and mutant IDH enzymes	13
Figure 6: Schematics showing the procedure of the suppressor screen	14
Figure 7: Schematics of CRASH-Assay (Anne E Dodson, Jasper Rine, 2015).....	17
Figure 8: Sensitizing conditions found.	20
Figure 9: Suppressors found.	21
Figure 10: One mutated gene responsible for growth phenotype	21
Figure 11: Complementation assay.....	22
Figure 12: Test for dominance.....	22
Figure 13: Deletion of <i>SET2</i> in a <i>dld2Δ</i> background phenocopies suppression phenotype.....	23
Figure 14: <i>RPD3</i> deletion in a <i>dld2Δdld3Δ</i> mutant leads to suppression phenotype.....	24
Figure 15: Acetylation levels of H4K12.....	24
Figure 16: Flow Cytometry.....	25

6 List of Tables

Table 1: Strains used in this study	18
Table 2: Oligonucleotides used in this study	19
Table 3: Carbon sources and stresses tested in the suppressor screen	20

7 Bibliography

Adam Cohen, Sheri Holmen, and Howard Colman, 2013. IDH1 and IDH2 Mutations in Gliomas. *Current Neurology and Neuroscience Reports*, May.

Anne E Dodson, Jasper Rine, 2015. Heritable capture of heterochromatin dynamics in *Saccharomyces cerevisiae*. *eLIFE*, January.

Anne E. Dodson, 2016. <https://escholarship.org>. [Online] Available at: <https://escholarship.org/uc/item/1zw9b27v> [Zugriff am November 2017].

Bourc'his D, 2010. Fundamentals of epigenetics. *Bulletin de l'Academie nationale de medicine*, February.pp. 271-81.

Charles S.Hoffman, Fred Winston, 1987. A ten-minute DNA preparation from yeast efficiently releases autonomous plasmids for transformiaon of *Escherichia coli*. *Gene*, May, Band 57, pp. 267-272.

De Rubertis F, Kadosh D, Henchoz S, Pauli D, Reuter G, Struhl K, Spierer P, 1996. The histone deacetylase RPD3 counteracts genomic silencing in *Drosophila* and yeast.. *Nature*, December.pp. 589-91.

Deborah M. Thurtle-Schmidt, Anne E. Dodson, and Jasper Rine, 2016. Histone Deacetylases with Antagonistic Roles in *Saccharomyces cerevisiae* Heterochromatin Formation. *Genetics*, September.p. 177–190.

Dodson A, Rine J, 2015. Heritable capture of heterochromatin dynamics in *Saccharomyces cerevisiae*.. *Elife*, January.

Ellahi A, Thurtle DM, Rine J., 2015. The Chromatin and Transcriptional Landscape of Native *Saccharomyces cerevisiae* Telomeres and Subtelomeric Domains.. *Genetics*, June.

Fabio Puddu, Tobias Oelschlaegel et al., 2015. Synthetic viability genomic screening defines Sae2 function in DNA repair. *EMBO*, April.

Garzon R, Fabbri M, Cimmino A, Calin GA, Croce CM., 2006. MicroRNA expression and function in cancer.. *Trends in molecular medicine*, December.

Goldstein AL, McCusker JH., 1999. Three new dominant drug resistance cassettes for gene disruption in *Saccharomyces cerevisiae*. *Yeast*, pp. 1541-53.

Gregory J. Kolb, Scott A. Jones, Matthew W. Donnelly, David Gorman, Robert Thomas., 2007. *Heliostat Cost Reduction Study*, Albuquerque, New Mexico 87185 and Livermore, California 94550: Sandia National Laboratories.

Grunstein M, Gasser SM., 2013. Epigenetics in *Saccharomyces cerevisiae*.. *Cold Spring Harbour perspectives in Biology*, July.

- Hecht A, Laroche T, Strahl-Bolsinger S, Gasser SM, Grunstein M., 1995. Histone H3 and H4 N-termini interact with SIR3 and SIR4 proteins: a molecular model for the formation of heterochromatin in yeast.. *The Cell*, February, pp. 583-92.
- Imai S, Armstrong CM, Kaeberlein M, Guarente L., 2000. Transcriptional silencing and longevity protein Sir2 is an NAD-dependent histone deacetylase.. *Nature*, February, pp. 795-800.
- Imai S, Guarente L, 2014. NAD⁺ and sirtuins in aging and disease.. *Trends in Cell Biology*, August.
- Jonathan Hodgkin, 2005. *Genetic suppression*. [Online]
Available at: http://www.wormbook.org/chapters/www_geneticsuppression/geneticsuppression.html
[Zugriff am November 2017].
- Jones PA, Takai D, 2001. The role of DNA methylation in mammalian epigenetics.. *Science*, pp. 1068-70.
- Lee JS, Shilatifard A., 2007. A site to remember: H3K36 methylation a mark for histone deacetylation.. *Mutation research*, May.
- Longtine MS1, McKenzie A 3rd, Demarini DJ, Shah NG, Wach A, Brachat A, Philippsen P, Pringle JR., 1998. Additional modules for versatile and economical PCR-based gene deletion and modification in *Saccharomyces cerevisiae*.. *Yeast*, pp. 953-61.
- Loo S, Rine J., 1994. Silencers and domains of generalized repression.. *Science*, June, pp. 1768-71.
- Ming Yang, Tomoyoshi Soga, Patrick J. Pollard, 2013. Oncometabolites: linking altered metabolism with cancer. *Journal of clinical investigation*, September, p. 3652–3658.
- National Cancer Institute, 2017. *PARP Inhibitors May Be Effective in Brain, Other Cancers with IDH Mutations*. [Online]
Available at: <https://www.cancer.gov/news-events/cancer-currents-blog/2017/idh-mutation-parp>
[Zugriff am 24 10 2017].
- Ralph J. DeBerardinis and Navdeep S. Chandel, 2016. Fundamentals of cancer metabolism. *Oncology*.
- Ramakrishnan V, 1997. Histone structure and the organization of the nucleosome.. *Annual review of Biophysics and biomolecular structure*, pp. 83-112.
- Rine J, Herskowitz I., 1987. Four genes responsible for a position effect on expression from HML and HMR in *Saccharomyces cerevisiae*.. *Genetics*, May, pp. 9-22.
- Robertson KD, Jones PA, 2000. DNA methylation: past, present and future directions.. *Carcinogenesis*, March, pp. 461-7.
- Ryan Janke, Anne E. Dodson, Jasper Rine, 2015. Metabolism and Epigenetics. *Annual Review of Cell and Developmental Biology*, September, p. 473–496. .
- Ryan Janke, Anthony T Iavarone, Jasper Rine, 2017. Oncometabolite D-2-Hydroxyglutarate enhances gene silencing through inhibition of specific H3K36 histone demethylases. *eLIFE*.

Shenghong Ma et al., 2015. D-2-hydroxyglutarate is essential for maintaining oncogenic property of mutant IDH-containing cancer cells but dispensable for cell growth. *Oncotarget*, April, Band 6, p. 8606–8620.

Shikhar Sharma, Theresa K. Kelly, and Peter A. Jones¹, 2009. Epigenetics in cancer. *Carcinogenesis*, September. p. 27–36.

Steakley DL, Rine J, 2015. On the Mechanism of Gene Silencing in *Saccharomyces cerevisiae*. *G3: Genes, Genomes, Genetics*, August.

STEPHEN E. RUNDLETT, ANDREW A. CARMEN, RYUJI KOBAYASHI[†], SERGEI BAVYKIN, BRYAN M. TURNER[‡], AND MICHAEL GRUNSTEIN, 1996. HDA1 and RPD3 are members of distinct yeast histone deacetylase complexes that regulate silencing and transcription. *Biochemistry*, December. p. 14503–14508.

Subhankar Biswas, C. Mallikarjuna Rao, 2017. Epigenetics in cancer: Fundamentals and Beyond. *Pharmacology and Therapeutics*, May. pp. 118-134.

Thurtle DM, Rine J., 2014. The molecular topography of silenced chromatin in *Saccharomyces cerevisiae*. *Genes and Development*, February. pp. 245-58.

Wach A, Brachat A, Pöhlmann R, Philippsen P, 1994. New heterologous modules for classical or PCR-based gene disruptions in *Saccharomyces cerevisiae*. *Yeast*, pp. 1793-808.

Xiao-Fen Chen, Benjamin Kuryan et al., 2012. The Rpd3 Core Complex Is a Chromatin Stabilization Module. *Current Biology*, January. pp. 56-63.